Published in final edited form as:
J Immunol. 2013 April 1; 190(7): 3438–3446. doi:10.4049/jimmunol.1203140.

Antigen-specific memory T_{reg} control memory responses to influenza virus infection

Erik L. Brincks[1], **Alan D. Roberts**[1], **Tres Cookenham**[1], **Stewart Sell**[2], **Jacob E. Kohlmeier**[3], **Marcia A. Blackman**[1], and **David L. Woodland**[4]
Trudeau Institute, Saranac Lake, NY 12983

Abstract

Regulatory $CD4^+FoxP3^+$ T cells (Treg) are key regulators of inflammatory responses and control the magnitude of cellular immune responses to viral infections. However, little is known about how Treg contribute to immune regulation during memory responses to previously-encountered pathogens. Here we utilized influenza $NP_{311-325}/IA^b$ Class II tetramers to track the antigen-specific Treg response to primary and secondary influenza virus infections. During secondary infections, antigen-specific memory Treg showed accelerated accumulation in the lung-draining lymph node and lung parenchyma relative to a primary infection. Memory Treg effectively controlled the *in vitro* proliferation of memory $CD8^+$ cells in an antigen-specific fashion that was MHC class II dependent. When memory Treg were depleted prior to secondary infection, the magnitude of the antigen-specific memory $CD8^+$ T cell response was increased, as was pulmonary inflammation and airway cytokine/chemokine expression. Replacement of memory Treg with naïve Treg failed to restore the regulation of the memory CD8 T cell response during secondary infection. Together, these data demonstrate the existence of a previously undescribed population of antigen-specific memory Treg that shape the cellular immune response to secondary influenza virus challenges and offer an additional parameter to consider when determining the efficacy of vaccinations.

INTRODUCTION

Regulatory $CD4^+FoxP3^+$ T cells (Treg) play important regulatory roles in the pathogenesis of cancer, autoimmune disease, and infectious disease. For example, in immune responses against tumors, Treg dampen tumor-specific immune responses both in the local tumor microenvironment and in secondary lymphoid organs, resulting in enhanced tumor survival and metastasis (1, 2). In contrast, aberrant Treg function can be observed in a number of autoimmune diseases—including systemic lupus erythematosis, multiple sclerosis, rheumatoid arthritis, and type 1 diabetes (3, 4). During the immune response to infection, Treg contribute to the resolution of inflammatory responses by limiting pro-inflammatory cytokine expression, by reducing inflammation in infected tissues, and by limiting pathogen-specific T cell responses (5–9). In many infections, Treg function is beneficial, as it limits immunopathology. However, Treg activity can also promote persistence of a pathogen, thereby turning what could be an acute/cleared infection into a chronic/persistent infection

Corresponding Author: Marcia A. Blackman, Trudeau Institute, 154 Algonquin Avenue, Saranac Lake, NY 12983, mblackman@trudeauinstitute.org. Phone: 518-891-3080.
[1]Trudeau Institute, 154 Algonquin Avenue, Saranac Lake, NY 12983
[2]Division of Translational Medicine, the Wadsworth Center, New York State Department of Health and the Department of Biomedical Sciences, School of Public Health, University at Albany, State University of New York, Albany, NY 12201
[3]Emory University School of Medicine, Department of Microbiology and Immunology, 1510 Clifton Road, Rollins Research Center, Rm 3133, Atlanta, GA 30322
[4]Keystone Symposia, PO Box 1630, Silverthorne, CO 80498

(5, 10–12). Determining the positive and negative roles Treg play in the pathogenesis of infections is critical for the understanding of disease progression, and will also provide insights for improving the design of vaccines against specific pathogens.

A role for T regulatory cells in the control of virus infections has been implicated for a number of viruses, including respiratory syncytial virus (6, 13), herpes simplex virus (9), rotavirus (14), dengue virus (15), and coronavirus (7, 16). There is increasing evidence that Treg can be pathogen-specific. For example, Treg antigen specificity has been implicated in *Toxoplasma gondii* (17) and *Leishmania major* infections (10, 18), where *in vitro* proliferation assays demonstrated that Treg responded to pathogen-specific simulation. Also, following adoptive transfer of P25 TCR transgenic Treg specific for a *Mycobacterium tuberculosis* (Mtb) antigen, there was antigen-specific proliferation to Mtb antigens and delayed effector responses at the site of infection (11). Most recently, MHC Class II tetramers specific for two epitopes expressed by the rJ2.2 strain of mouse hepatitis virus were used to identify virus-specific Treg that were recruited during infection and contributed to regulation of effector responses (7). These data support the contribution of antigen-specific Treg in primary infections. However, little is known about the contribution of Treg to memory responses. Key questions are whether antigen-specific Treg develop into a memory population and whether they play a role in regulating recall responses.

Here, we examined memory responses to influenza virus using MHC Class II tetramers to track antigen-specific CD4 T cell responses. The data indicate that antigen-specific Treg were recruited to the lungs during secondary infection and that the rate of recruitment was enhanced compared to a primary response. This memory Treg response influenced pulmonary inflammation and regulated antigen-specific CD8 T cell recall responses both *in vitro* and *in vivo*. The *in vitro* studies showed that regulation of memory CD8 T cell proliferation required MHC Class II expression on antigen presenting cells and was pathogen-specific. Further, adoptive transfer of naïve Treg cells failed to regulate the recall response of memory CD8 T cells specific for influenza virus. Together, these data support the existence of antigen-specific memory Treg cells that play an important role in the regulation of immune responses to secondary infections.

MATERIALS AND METHODS

Mice

C57BL/6, B6.SJL-Ptprca Pep3/BoyJ (CD45.1), and B6.PL-Thy1a/Cy (CD90.1+) mice were purchased from the Trudeau Institute. Foxp3^{gfp} mice on a B6 background were provided by A. Rudensky (University of Washington, Seattle, WA). FoxP3-DTR mice on a B6 background were previously described (31) and provided by T. Sparwasser (Institute of Infection Immunology, TWINCORE, Center for Experimental and Clinical Infection Research, Hannover, Germany). Vert-X (C57BL/6 IL-10/eGFP reporter) mice were provided by M. Mohrs (Trudeau Institute). All animal studies have been reviewed and approved by the Trudeau Institute Animal Care and Usage Committee.

Viruses and infections

Influenza viruses A/HK-x31 (x31, H3N2) and A/PR8 (PR8, H1N1) were grown, stored, and titered as previously described (32). For virus infection, mice were anesthetized with 2,2,2-tribromoethanol (200 mg/kg) and virus was administered intranasally (500 50% egg infectious doses [EID_{50}] for primary PR8 infections, 300 EID_{50} for x31 infections, 5×10^4 EID_{50} for secondary PR8 infections, 3×10^5 EID_{50} for secondary x31 infections, and 250 EID_{50} for Sendai). In vitro infections were completed as described previously (33). Briefly, cells were co-incubated with a 10MOI dose of virus for 30 minutes on ice, followed by 30

minutes at 37°C. Cells were washed 2X with complete medium and cultured in 96 well plates.

Tissue harvest and flow cytometry

Mice were sacrificed at the indicated times and cells were isolated from the lung airways by bronchoalveloar lavage (BAL), the lung parenchyma by digestion in collagenase / DNase for 1 hour at 37°C followed by percoll gradient centrifugation, and the MLN and spleen by mechanical disruption. Following red blood cell lysis with ammonium buffered chloride, live cell numbers were determined by counting and trypan blue exclusion (32). Single cell suspensions were incubated with Fc-block (anti-CD16/32) for 15 minutes on ice followed by staining with influenza $NP_{311\text{-}325}$ $I(A)^b$, $FluNP_{366\text{-}374}D^b$, $FluPA_{224\text{-}233}D^b$, or $SenNP_{324\text{-}332}K^b$ tetramers for 1 hour at room temperature. Tetramers were obtained from the NIH Tetramer Core Facility (http://tetramer.yerkes.emory.edu/) or from the Trudeau Institute Molecular Biology Core (http://www.trudeauinstitute.org). Tetramer-labeled cells were stained with antibodies to CD4, CD8, CD25, CD44, CD45.1, CD45.2, CD69, CD90.1, CTLA4, GITR (BD Bioscience and eBiosciences). For intracellular FoxP3 staining, cells were fixed, permeablized, and stained according to FoxP3 Staining Kit protocol (ebioscience). Samples were acquired on a FACSCanto II flow cytometer (BD Biosciences) and data were analyzed with FlowJo software (Tree Star).

Assessment of cytokine production by intracellular cytokine staining

For $CD8^+$ T cell cytokine production, single cell suspensions were incubated with influenza $NP_{366\text{-}374}$ or influenza $PA_{224\text{-}232}$ peptides as previously described (34). Cells were stained for surface markers, fixed, and permeabilized (CytoFix/CytoPerm kit, BD Biosciences), and stained with monoclonal antibodies to IFNγ. For $CD4^+$ T cell cytokine production, single cell suspensions were incubated with influenza $NP_{311\text{-}325}$ peptide. Cells were stained for surface markers, fixed, and permeabilized with FoxP3 Staining Kit (ebioscience), and stained with monoclonal antibodies for IL-10, TGFβ, CTLA4, IFNγ, and TNFα (BD Biosciences, ebioscience, R&D).

Measurement of proliferation by BrdU incorporation

Measurement of proliferation by BrdU incorporation was done similarly to previously described (35). Briefly, mice were administered BrdU (200 μl of a 4 mg/ml solution in PBS) i.p. and maintained on drinking water containing BrdU (0.8 mg/ml) for 24 h before harvest. Single cell suspensions were stained with tetramers and Abs to surface proteins as described above and BrdU incorporation was detected using the BrdU Flow Kit (BD Biosciences).

In vitro suppression assay

$CD4^+$ T cells were enriched by negative magnetic selection from influenza-primed *Foxp3*^{gfp} mice (pooled from 10 mice at day 35 post-infection) using a mouse $CD4^+$ T cell BD iMag enrichment kit (BD Bioscience). After enrichment of $CD4^+$ T cells, $CD4^+GFP^-$ and $CD4^+GFP^+$ T cells were then sorted using a BD FACSVantage cell sorter (BD). For the suppression assay, $3–5 \times 10^4$ CFSE-labeled (3 μM; Invitrogen) memory $CD8^+$ T cells from influenza-infected CD90.1 mice were co-cultured with varying ratios of T reg cells and 10^5 $CD45.1^+$ antigen presenting cells (APC) per well in a 96-well round bottom plate. APC had been infected with 10 MOI of influenza virus 24 hours prior to co-cultures. In some cultures, Treg sorted from influenza-infected mice were used in cultures with memory $CD8^+$ T cells from Sendai virus-infected CD90.1 mice and APC that had been infected in vitro with 10 MOI of Sendai virus. After 90 h, cells were harvested, stained with MHC Class I tetramers, and stained for congenic surface markers and CD8. $CD4^+Foxp3^-$ responder cells were analyzed for CFSE dilution by flow cytometry.

Measurement of morbidity and airway resistance

Enhanced pause (Penh) was measured using a whole body plethysmograph similar to previously described (36) (Buxco Electronics, Sharon, CT). Penh values were recorded daily following secondary influenza virus infection. Breathing patterns were recorded for 10 minutes per mouse to obtain an average Penh value. To determine morbidity, mice were weighed daily.

Measurement of airway cytokine and chemokine expression

BAL fluid was harvested from mice 5 days after secondary influenza virus challenge. Subsequently, the cytokine and chemokine expression was determined using a mouse cytokine/chemokine multiplex (Invitrogen, Carlsbad, CA).

Histological analysis

Lungs were inflated with 5 ml neutral buffered formalin (10% vol/vol) via the trachea and fixed for 72 h. Lungs were embedded in paraffin wax, and 4–5-μm sections were mounted onto slides and stained with hematoxylin and eosin. The inflammatory response and proliferation were assessed and scored according to scales depicted and described in Supplemental Figures 3A and 3B by a pathologist who was blinded as to the identity of the samples. All slides were viewed with an Axioplan 2 microscope and images were recorded with a Zeiss AxioCam digital camera (both from Carl Zeiss, Inc.).

Statistical analysis

Statistical analysis was performed using Prism 5 (GraphPad Software). Significance was determined by an unpaired two-tailed Student's t test or by two-way ANOVA with subsequent Bonferroni post hoc tests. P-values less than 0.05 were considered significant.

RESULTS

Primary and secondary influenza virus infections induce the recruitment of antigen-specific T_{reg} to the lung and lung-draining lymph node

To assess the recruitment of Treg during the primary and recall responses to influenza virus, mice were infected with H1N1 influenza virus (A/PR8, PR8) to analyze the primary infection or were infected with H3N2 influenza virus (A/HK-x31, X31) and challenged with PR8 to analyze the recall response. At various days after infection or challenge, the Treg ($CD4^+FoxP3^+$) response was quantified in the lung and lung-draining lymph node. Consistent with cellular responses to other virus infections, Treg accumulated transiently at the site of infection as well as in the tissue-draining lymph node (Figure 1). Treg recruitment to the lung-draining lymph node was accelerated during the response to secondary challenge, and more Treg were recruited to both the lung and the lung-draining lymph node during responses to secondary challenge (Figure 1A and 1E). To assess the antigen-specificity of the Treg response, CD4 cells were stained with MHC Class II $I\text{-}A^b$ tetramer specific for the influenza $NP_{311\text{-}324}$ epitope (Figure 1B and 1F). Compared with naïve mice, mice previously infected with influenza virus had an expanded antigen-specific Treg compartment prior to infection (Figure 1B and 1F). As shown in Figure 1C and 1G, antigen-specific Treg accumulated in the lung and lung-draining lymph node during both primary and secondary challenge. These antigen-specific Treg expressed molecules consistent with Treg phenotype and function, including CD25, CTLA4, and GITR (Supplemental Figure 1). We were unable to detect IL-10 expression in the Treg responding to secondary challenge, though IL-10 transcription was detected in Treg during the response to primary infection (Supplemental Figure 1). Interestingly, antigen-specific Treg accumulated with accelerated kinetics during the response to secondary influenza virus infection relative to the response

against primary infection. Also of note, the kinetics of the antigen-specific Treg response were distinct from the kinetics of antigen-specific $CD4^+FoxP3^{neg}$ cells—i.e. the peak of the antigen-specific Treg response occurred earlier than the peak of the antigen-specific CD4 effector response (Figure 1D and 1H). Consistent with previous reports of antigen-specific responses correlating with increased proliferation, the majority of antigen-specific Treg had proliferated in response to infection (Supplemental Figure 2). Together, these data suggest that antigen-specific Treg are involved in the primary and recall responses to influenza virus infection, and the accelerated recruitment during recall responses suggests the existence of a population of antigen-specific memory Treg that persists in the host.

Memory T_{reg} regulate *in vivo* inflammation during the recall response to influenza virus infection

The pulmonary immune response to secondary influenza infections involves not only an antigen-specific T cell response, but also an inflammatory response characterized by chemokine and cytokine production as well as alterations to the pulmonary architecture. To assess the role of memory Treg cells in regulating pulmonary inflammation, mice were infected with X31 and challenged with PR8, with or without anti-CD25 mAb treatment prior to challenge. This treatment resulted in a depletion of 70–80% of the existing $FoxP3^+CD4^+$ Treg cells (data not shown). Scoring of histology sections revealed increased inflammation and epithelial proliferation in the mice that had been depleted of Treg cells (Figure 2A & 2B). Grading of inflammation is based on both the nature of the lesion and the degree of involvement (Supplemental Figure 3A). Inflammation consists of a mixed mononuclear cell infiltrate which varies from small compact foci through large dense areas, (Supplemental Figure 3A). Similar dense areas of lymphoid tissue have been seen in chronic lung infections in humans and have been identified as bronchus-associated lymphoid tissue (BALT) (19). BALT is also seen in mice with repeated virus infections of the lung (20). The conversion of areas of the lung next to bronchi into BALT is much greater in mice depleted of Tregs than in mice with Tregs, which feature loose collections of large monocytes with retention of alveolar structure.

Even more impressive are large areas in which the alveolar spaces were filled with epithelial cells (Supplemental Figure 3B). As indicated by the proliferation score, proliferation of type II pneumocytes was much greater in mice depleted of Tregs (Figure 2A & 2C). It is well-documented that such proliferation is seen in mice infected with flu virus beginning with 3–6 days after primary infection, (21) and peaking in the alveoli at about 2 weeks (21–23). As stated by Straub in 1937 (24): “A chronic reparative process in surviving mice has, indeed, been regularly met with. This is not, as so often in man, fibrous but epithelial in nature. The epithelium of the terminal bronchioles proliferates and becomes more or less stratified…. The proliferation does not stop here, but regularly invades the lung tissue. It first enters the respiratory bronchioles and next the alveoli.” In the absence of Treg, this exaggerated repair response expands to occupy more than 50% of the lung tissue on histologic slides. Squamous metaplasia was not seen, most likely as it was only 5 days after secondary infection.

Treg depletion did not alter morbidity (Figure 2E), mortality, or virus clearance, but did result in increased PenH compared to the isotype-treated mice (Figure 2D)—suggesting that the lungs of depleted mice had increased pathology and decreased lung function. Consistent with the H&E scoring and the PenH evaluations, mice depleted of Treg had increased pulmonary chemokine (IP-10 and MIG) and cytokine (IL-6 and IFNγ) expression compared to isotype control-treated mice (Figure 2F–I). Together, these data suggest that memory Treg contribute to the control of pulmonary inflammation during the recall response to secondary challenge.

Memory T_{reg} regulate the *in vivo* memory CD8 T cell response to influenza virus infection

To complement the studies of pulmonary inflammation induced by influenza virus infection, the role of memory Treg in controlling secondary influenza infection was investigated. Mice were infected with X31 and challenged 35 days later with PR8, with anti-CD25 mAb (PC61) or isotype control antibody for 2 days prior to challenge. Five days post-PR8 challenge, the influenza-specific CD8 T cell response was measured using MHC Class I tetramers specific for two immunodominant influenza virus epitopes, nucleoprotein ($NP_{366-374}/D^b$) and acid polymerase ($PA_{224-233}/D^b$) (Figure 3A). Depletion of Treg increased the magnitude of the pulmonary tetramer-specific CD8 T cell response (Figure 3B, C), and more of these CD8 T cells produced interferon-γ during the recall response (Figure 3D, E). These data support a role for memory Treg in controlling the *in vivo* memory CD8 T cell response to secondary influenza virus infection.

The functional regulation of memory responses suggests that memory Treg are maintained after a primary infection. However, an alternative explanation is that memory CD8 T cells are more susceptible to regulation by Treg than naïve T cells. That is, memory CD8 T cell responses to secondary infection could be similarly regulated by any Treg population responding to infection—be they antigen-inexperienced Treg or memory Treg. To compare the function of memory Treg and naïve Treg in regulating a memory CD8 T cell response, we utilized the FoxP3-DTR mice, in which cells expressing FoxP3 also express the diphtheria toxin receptor on their cell surface. To deplete memory Treg, FoxP3-DTR mice previously infected with influenza virus were treated with diphtheria toxin prior to secondary infection (Figure 4A). Diphtheria toxin treatment depleted both tetramer-positive and tetramer-negative $FoxP3^+$ cells while leaving the antigen-specific $CD4^+FoxP3^{neg}$ cells intact in both the lung and the lung-draining lymph node (Figure 4B and 4C). Similar to the results observed using PC61 mAb treatment to deplete memory Treg, the depletion of Treg by diphtheria toxin resulted in an increased antigen-specific CD8 T cell response at day 5 post-infection (Figure 4D, E). In contrast, the adoptive transfer of naïve Treg (to replace the depleted memory Treg, Figure 4B and 4C) resulted in CD8 T cell responses similar to those in mice that had no Treg (Figure 4D, E). Only in mice in which the memory Treg population had not been depleted was the antigen-specific CD8 T cell response to secondary infection reduced. This regulatory function, together with the accelerated recruitment kinetics observed in Figure 1, suggest that influenza virus infection results in the formation of a pool of memory Treg with the capacity to regulate immune responses to subsequent challenge with virus in an antigen-specific fashion. Considered together, the antibody depletion and diphtheria toxin depletion data suggest that antigen-specific memory Treg, and not naïve Treg, are important players in the control of pulmonary inflammation and the regulation of memory CD8 T cell responses.

Memory Treg regulate proliferation of memory CD8 T cells in an antigen-specific fashion that requires MHC Class II

A defining characteristic of T regulatory cells is their ability to regulate immune responses, including their ability to inhibit the proliferation of CD8 T cells that have been stimulated through their T cell receptor with anti-CD3 or with antigen. To complement *in vivo* studies of the influenza-specific memory Treg function, we isolated memory Treg from influenza-infected mice and used them to inhibit the proliferation of memory CD8 T cells stimulated *in vitro* by co-culture with infected antigen presenting cells (see Supplemental Figure 4 for outline of experimental design, cell sources, and culture combinations). When the cultures contained only memory CD8 T cells and APC, significant CD8 T cell proliferation was observed. When memory $CD4^+FoxP3^+$ Treg, but not memory $CD4^+FoxP3^{neg}$ cells, were added to the CD8/APC co-cultures, proliferation of the memory CD8 T cells was significantly decreased (Figures 5A and 5B). Increasing the ratio of influenza NP_{366}-specific

CD8 memory cells to influenza-specific Treg (culture + Treg in Figure 5C) resulted in the decrease and eventual loss of inhibitory effect of the memory Treg cells. In contrast, altering the ratio of NP_{366}-specific CD8 memory cells to influenza-specific $CD4^{+}FoxP3^{neg}$ cells (Culture + CD4 in Figure 5C) in the cultures did not influence the proliferation of the CD8 effectors.

To assess the pathogen specificity of the inhibitory function of the memory Treg, the effect of influenza-specific Treg cells on the ability of Sendai-virus-infected APC to stimulate the proliferation of Sendai virus NP_{324}-specific memory CD8 cells. The populations of influenza-specific memory Treg and memory CD4 effectors (i.e. those that were used in Figure 5A–C) were used to inhibit the proliferation of Sendai virus NP_{324}-specific CD8 effectors. Neither the addition of influenza-specific memory Treg nor the addition of influenza-specific CD4 effectors influenced the proliferation by the Sendai virus NP_{324}-specific CD8 T cells (Figure 5D). Furthermore, altering the ratio of CD8 effectors to Treg cells did not influence the proliferation. Together with the data from Figure 5C, these data support a model in which the inhibitory function by memory Treg cells requires recognition of cognate antigen.

To investigate the requirement for MHC class II in Treg function, CD8/APC/Treg cultures were set up using APC from MHC Class II-deficient mice. In the absence of MHC Class II on the influenza-infected APC to present antigens to CD4 cells, there was no inhibition of CD8 proliferation by the influenza-specific memory Treg (Figure 5E). Of note, Treg harvested from infected lungs, from the lung-draining lymph node, or from the spleen all had similar capacity to inhibit memory CD8 T cell proliferation (Figure 5E). Together, these data demonstrate that influenza-specific memory Treg regulate the recall response of memory CD8 T cells in a pathogen-specific, MHC Class II dependent manner.

DISCUSSION

There are two possible models for Treg control of CD8 T cell function- an indirect two-step model involving antigen presenting cells, or a direct model. The requirement for MHC ClassII expression on antigen presenting cells supports the possibility that interactions between memory Treg and antigen presenting cells could lead to deactivation of the antigen presenting cell. These interactions could take place in the lung-draining lymph node or in the infected lung environment, as recall responses include activation of T cells in both. Such a model would be consistent with reports that Treg:DC interactions can alter subsequent immune responses (25, 26). Alternatively, memory Treg might interact directly with memory CD8 T cells to inhibit their proliferation (27, 28).

In a two-step model of Treg function, memory Treg would interact with APC expressing influenza antigens, thereby activating the Treg. Subsequently, the activated memory Treg, or soluble factors secreted by these Treg, would interact with the CD8 T cells, thereby blocking their proliferation. During the recall response the antigen-specific Treg expressed surface markers consistent with regulatory function (29) (e.g. CD25, CTLA-4, GITR), but we were unable to detect the production of IL-10, IFNγ, TGFβ, or TNFα in these cells after stimulation with antigen. The lack of cytokine production suggests that their regulatory function is via a cell-contact dependent mechanism. While the specific mechanisms of regulation have not been explicitly determined, prior studies of Treg regulatory mechanisms suggest that multiple mechanisms likely contribute to the regulation (e.g. CTLA-4, TRAIL, etc.) (29, 30).

Measuring Treg function commonly involves using Treg to block proliferation of CD8 stimulated with anti-CD3/anti-CD28 stimulation or with PMA/ionomycin stimulation of the

cells in culture (7, 9, 10). Contrary to previous investigations of infection, the present study used a more physiological approach in which Treg were used to block memory CD8 T cell proliferation that was stimulated by influenza-infected antigen presenting cells. Utilizing this pathogen-specific assay, we found that memory Treg from an influenza-primed host effectively suppressed the proliferation of influenza-specific memory CD8 T cells stimulated with influenza-infected APC. However, when those same influenza-specific Treg were placed into cultures with Sendai virus infected APC presenting to Sendai-specific CD8 memory cells, the Treg failed to block proliferation—suggesting that the regulatory functions of Treg are pathogen specific. Further, Treg function also appears to require TCR stimulation, as the absence of MHC Class II expression on the influenza-infected antigen presenting cells resulted in minimal regulation of CD8 proliferation by the memory Treg cells. These data suggest that Treg require TCR stimulation for optimal activity and that the regulatory functions of Treg might be more restricted than previously suggested by data from cultures using anti-CD3/anti-CD28 stimulation of CD8 T cells. In those experiments, the antibodies used to trigger CD8 effector proliferation would also stimulate Treg activation in a non-specific fashion. Future studies should take this potential complicating factor into consideration and more specifically examine the requirement for antigen-specific Treg activation when assessing Treg function *in vitro*.

Our findings have substantial implications for vaccination strategies, as we were also able to find antigen-specific memory Treg populations after whole-protein vaccination with influenza NP (data not shown). Eliciting an antigen-specific Treg response could be beneficial during influenza virus infections as well as other infections where immunopathology is a concern, including coronavirus (7, 16), dengue virus (15), and respiratory syncytial virus (6, 13). Vaccination attempts to limit pathology in autoimmune disease could aim to elicit antigen specific Treg responses, though identifying target antigens would be an obvious obstacle in the context of autoimmunity (3, 4). In the context of tumor immunology, the activation of Treg during protein vaccinations against tumor antigens would be a serious concern, as multiple tumor models have demonstrated that Treg limit the efficacy of immunotherapy efforts (1, 2). Clearly, future studies of vaccination strategies need to consider potential vaccine-specific Treg responses and how such responses might influence the desired effect of the vaccine.

Taken together, our findings suggest a previously unappreciated population of antigen-specific memory Treg cells that regulate immune responses during secondary encounters with pathogens. While Treg have been recognized as cells that are constitutively activated and can rapidly respond to inflammation, we propose that the requirement of antigen recognition provides a critical checkpoint to Treg activation and subsequent regulatory function. During secondary infection, Treg suppression of immune responses is not global; rather, Treg activation is specific to the pathogen and results in regulation of pathogen specific responses. Thus, secondary infection with a pathogen stimulates a memory T cell response that rapidly and vigorously controls the pathogen while concomitantly stimulating a memory Treg response that rapidly and vigorously controls the immune response and limits immunopathology.

Supplementary Material

Refer to Web version on PubMed Central for supplementary material.

Acknowledgments

This work was supported by National Institutes of Health grants AI076499 (D.L.W and M.A.B.) and T32 AI049823 (D.L.W.), and funds from the Trudeau Institute.

The authors thank the Trudeau Institute Molecular Biology Core for the production of MHC I and MHC II tetramers, the NIH Tetramer Core Facility for the production of MHC II tetramers, Mike Tighe for sectioning and microscopy assistance, and Brandon Sells and Ron Lacourse for cell sorting.

Non-standard Abbreviations

Treg	regulatory T cell
dLN	draining lymph node

References

1. Cote AL, Usherwood EJ, Turk MJ. Tumor-specific T-cell memory: clearing the regulatory T-cell hurdle. Cancer Res. 2008; 68:1614–1617. [PubMed: 18339838]
2. Curiel TJ. Tregs and rethinking cancer immunotherapy. J Clin Invest. 2007; 117:1167–1174. [PubMed: 17476346]
3. Buckner JH. Mechanisms of impaired regulation by CD4(+)CD25(+)FOXP3(+) regulatory T cells in human autoimmune diseases. Nat Rev Immunol. 2010; 10:849–859. [PubMed: 21107346]
4. Long SA, Buckner JH. CD4+FOXP3+ T regulatory cells in human autoimmunity: more than a numbers game. J Immunol. 2011; 187:2061–2066. [PubMed: 21856944]
5. Belkaid Y, Rouse BT. Natural regulatory T cells in infectious disease. Nat Immunol. 2005; 6:353–360. [PubMed: 15785761]
6. Fulton RB, Meyerholz DK, Varga SM. Foxp3+ CD4 regulatory T cells limit pulmonary immunopathology by modulating the CD8 T cell response during respiratory syncytial virus infection. J Immunol. 2010; 185:2382–2392. [PubMed: 20639494]
7. Zhao J, Zhao J, Fett C, Trandem K, Fleming E, Perlman S. IFN-gamma-and IL-10-expressing virus epitope-specific Foxp3(+) T reg cells in the central nervous system during encephalomyelitis. J Exp Med. 2011; 208:1571–1577. [PubMed: 21746812]
8. Suvas S, Azkur AK, Kim BS, Kumaraguru U, Rouse BT. CD4+CD25+ regulatory T cells control the severity of viral immunoinflammatory lesions. J Immunol. 2004; 172:4123–4132. [PubMed: 15034024]
9. Suvas S, Kumaraguru U, Pack CD, Lee S, Rouse BT. CD4+CD25+ T cells regulate virus-specific primary and memory CD8+ T cell responses. J Exp Med. 2003; 198:889–901. [PubMed: 12975455]
10. Belkaid Y, Piccirillo CA, Mendez S, Shevach EM, Sacks DL. CD4+CD25+ regulatory T cells control Leishmania major persistence and immunity. Nature. 2002; 420:502–507. [PubMed: 12466842]
11. Shafiani S, Tucker-Heard G, Kariyone A, Takatsu K, Urdahl KB. Pathogen-specific regulatory T cells delay the arrival of effector T cells in the lung during early tuberculosis. J Exp Med. 2010; 207:1409–1420. [PubMed: 20547826]
12. Suvas S, Rouse BT. Treg control of antimicrobial T cell responses. Curr Opin Immunol. 2006; 18:344–348. [PubMed: 16616481]
13. Lee DC, Harker JA, Tregoning JS, Atabani SF, Johansson C, Schwarze J, Openshaw PJ. CD25+ natural regulatory T cells are critical in limiting innate and adaptive immunity and resolving disease following respiratory syncytial virus infection. J Virol. 2010; 84:8790–8798. [PubMed: 20573822]
14. Kim B, Feng N, Narvaez CF, He XS, Eo SK, Lim CW, Greenberg HB. The influence of CD4+ CD25+ Foxp3+ regulatory T cells on the immune response to rotavirus infection. Vaccine. 2008; 26:5601–5611. [PubMed: 18725261]
15. Dejnirattisai W, Duangchinda T, Lin CL, Vasanawathana S, Jones M, Jacobs M, Malasit P, Xu XN, Screaton G, Mongkolsapaya J. A complex interplay among virus, dendritic cells, T cells, and cytokines in dengue virus infections. J Immunol. 2008; 181:5865–5874. [PubMed: 18941175]
16. Trandem K, Anghelina D, Zhao J, Perlman S. Regulatory T cells inhibit T cell proliferation and decrease demyelination in mice chronically infected with a coronavirus. J Immunol. 2010; 184:4391–4400. [PubMed: 20208000]

17. Oldenhove G, Bouladoux N, Wohlfert EA, Hall JA, Chou D, Dos Santos L, O'Brien S, Blank R, Lamb E, Natarajan S, Kastenmayer R, Hunter C, Grigg ME, Belkaid Y. Decrease of Foxp3+ Treg cell number and acquisition of effector cell phenotype during lethal infection. Immunity. 2009; 31:772–786. [PubMed: 19896394]
18. Suffia IJ, Reckling SK, Piccirillo CA, Goldszmid RS, Belkaid Y. Infected site-restricted Foxp3+ natural regulatory T cells are specific for microbial antigens. J Exp Med. 2006; 203:777–788. [PubMed: 16533885]
19. Tschernig T, Pabst R. Bronchus-associated lymphoid tissue (BALT) is not present in the normal adult lung but in different diseases. Pathobiology. 2000; 68:1–8. [PubMed: 10859525]
20. Chen HD, Fraire AE, Joris I, Welsh RM, Selin LK. Specific history of heterologous virus infections determines anti-viral immunity and immunopathology in the lung. Am J Pathol. 2003; 163:1341–1355. [PubMed: 14507643]
21. Nelson AA, Oliphant JW. Histopathological changes in mice inoculated with influenza virus. Public Health Reports (1896–1970). 1939:2044–2054.
22. Dubin IN. A Pathological Study of Mice Infected with the Virus of Swine Influenza. Am J Pathol. 1945; 21:1121–1141. [PubMed: 19970853]
23. LOOSLI CG. The pathogenesis and pathology of experimental air-borne influenza virus A infections in mice. J Infect Dis. 1949; 84:153–168. [PubMed: 18113780]
24. Straub MJ. The microscopial changes in the lungs of mice infected with influenza virus. Pathology. 1937; 45:75–78.
25. Mahnke K, Bedke T, Enk AH. Regulatory conversation between antigen presenting cells and regulatory T cells enhance immune suppression. Cell Immunol. 2007; 250:1–13. [PubMed: 18313653]
26. Tang Q, Adams JY, Tooley AJ, Bi M, Fife BT, Serra P, Santamaria P, Locksley RM, Krummel MF, Bluestone JA. Visualizing regulatory T cell control of autoimmune responses in nonobese diabetic mice. Nat Immunol. 2006; 7:83–92. [PubMed: 16311599]
27. Chen ML, Pittet MJ, Gorelik L, Flavell RA, Weissleder R, von Boehmer H, Khazaie K. Regulatory T cells suppress tumor-specific CD8 T cell cytotoxicity through TGF-beta signals in vivo. Proc Natl Acad Sci U S A. 2005; 102:419–424. [PubMed: 15623559]
28. May KF Jr, Chang X, Zhang H, Lute KD, Zhou P, Kocak E, Zheng P, Liu Y. B7-deficient autoreactive T cells are highly susceptible to suppression by CD4(+)CD25(+) regulatory T cells. J Immunol. 2007; 178:1542–1552. [PubMed: 17237403]
29. Vignali DA, Collison LW, Workman CJ. How regulatory T cells work. Nat Rev Immunol. 2008; 8:523–532. [PubMed: 18566595]
30. Pillai MR, Collison LW, Wang X, Finkelstein D, Rehg JE, Boyd K, Szymczak-Workman AL, Doggett T, Griffith TS, Ferguson TA, Vignali DA. The plasticity of regulatory T cell function. J Immunol. 2011; 187:4987–4997. [PubMed: 22013112]
31. Lahl K, Loddenkemper C, Drouin C, Freyer J, Arnason J, Eberl G, Hamann A, Wagner H, Huehn J, Sparwasser T. Selective depletion of Foxp3+ regulatory T cells induces a scurfy-like disease. J Exp Med. 2007; 204:57–63. [PubMed: 17200412]
32. Kohlmeier JE, Reiley WW, Perona-Wright G, Freeman ML, Yager EJ, Connor LM, Brincks EL, Cookenham T, Roberts AD, Burkum CE, Sell S, Winslow GM, Blackman MA, Mohrs M, Woodland DL. Inflammatory chemokine receptors regulate CD8(+) T cell contraction and memory generation following infection. J Exp Med. 2011; 208:1621–1634. [PubMed: 21788409]
33. Brincks EL, Kucaba TA, Legge KL, Griffith TS. Influenza-induced expression of functional tumor necrosis factor-related apoptosis-inducing ligand on human peripheral blood mononuclear cells. Hum Immunol. 2008; 69:634–646. [PubMed: 18723061]
34. Brincks EL, Katewa A, Kucaba TA, Griffith TS, Legge KL. CD8 T cells utilize TRAIL to control influenza virus infection. J Immunol. 2008; 181:4918–4925. [PubMed: 18802095]
35. Kohlmeier JE, Connor LM, Roberts AD, Cookenham T, Martin K, Woodland DL. Nonmalignant clonal expansions of memory CD8+ T cells that arise with age vary in their capacity to mount recall responses to infection. J Immunol. 2010; 185:3456–3462. [PubMed: 20720204]

36. Brincks EL, Gurung P, Langlois RA, Hemann EA, Legge KL, Griffith TS. The magnitude of the T cell response to a clinically significant dose of influenza virus is regulated by TRAIL. J Immunol. 2011; 187:4581–4588. [PubMed: 21940678]

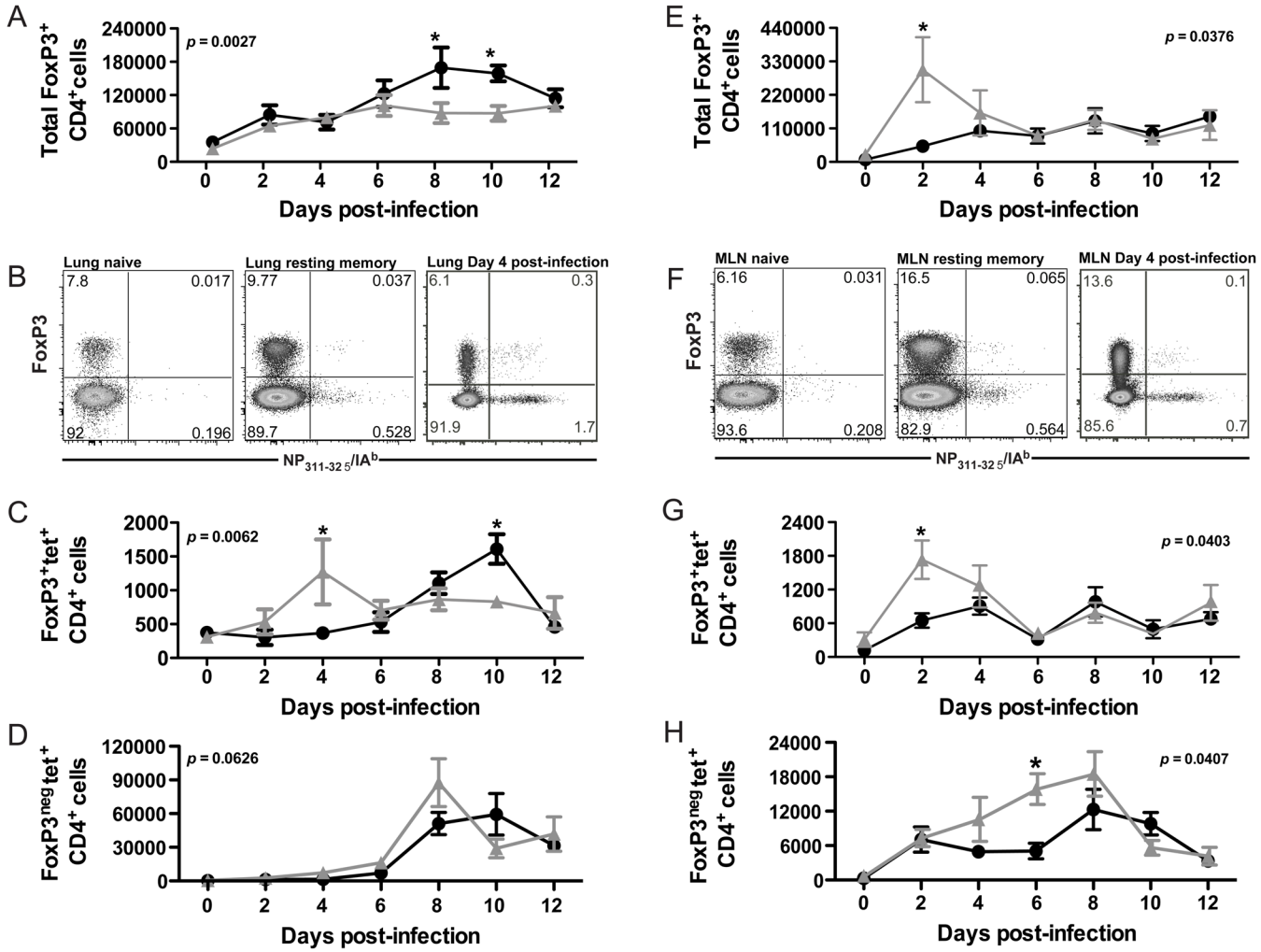

Figure 1. Influenza virus infection induces recruitment of antigen-specific T regulatory cells to the lung and lung-draining lymph node

C57BL/6 mice were sacrificed at indicated times after primary (600 EID_{50} PR8 influenza virus) or secondary (60,000 EID_{50} PR8 influenza virus) infection and lymphocytes harvested from the lung (A–D) or the lung-draining lymph node (E–H) were stained for CD4, FoxP3, and NP_{311}/I-A^b tetramer. *(A and E)* Total Treg $CD4^+FoxP3^+$ cells per lung (A) or draining lymph node (E) at various days after primary (●) or secondary (Δ) infection. *(B and F)* Representative plots from the lung (B) and dLN (F) gated on total $CD4^+$ cells in tissue. *(C and G)* Antigen-specific Treg NP_{311}/I-$A^{b+}CD4^+FoxP3^+$ cells per lung (C) or draining lymph node (G) at various days after primary (●) or secondary (Δ) infection. *(D and H)* Antigen-specific Treg NP_{311}/I-$A^{b+}CD4^+FoxP3^{neg}$ cells per lung (D) or draining lymph node (H) at various days after primary (●) or secondary (Δ) infection. For A, C, D, E, G, and H, significance was determined utilizing a two-way ANOVA. Subsequent analysis of individual timepoint significance was determined by Bonferroni post hoc tests; significance (*) indicates $p < 0.05$. Data are from four to five mice per time point in two independent experiments. Error bars indicate mean ± SD.

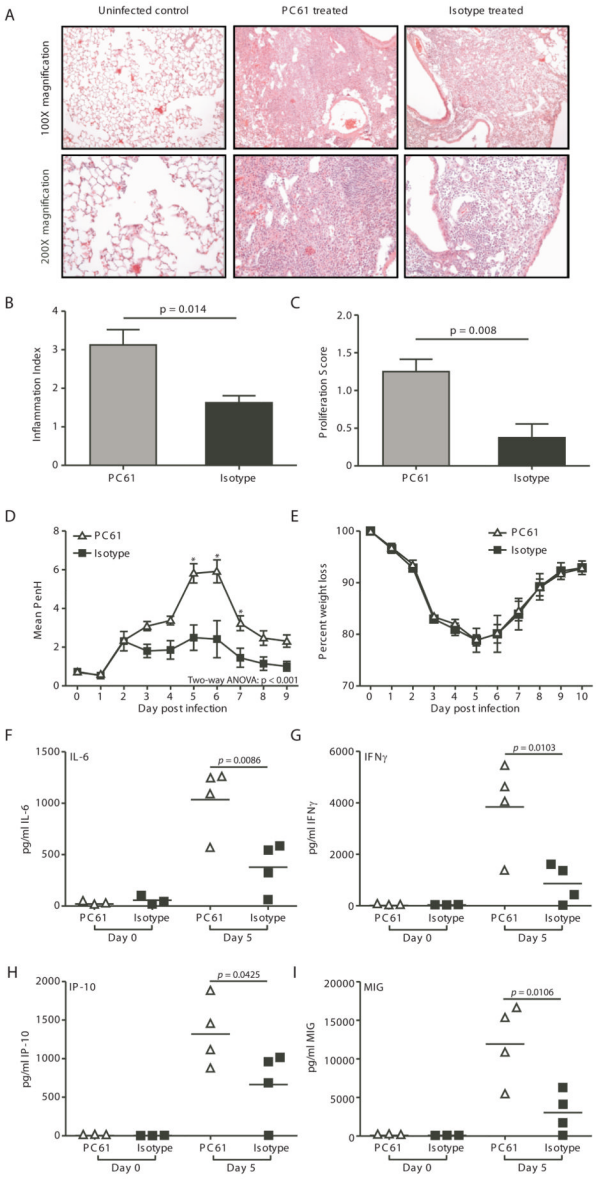

Figure 2. Depletion of Treg populations during influenza virus infection results in increased pulmonary inflammation

C57BL/6 mice were infected with 3000 EID_{50} x31 influenza virus and allowed to rest for 35 days. Mice were treated with PC61 or isotype control, then challenged with 60,000 EID_{50} PR8 influenza virus. On day 5 post-infection, whole lungs were harvested, fixed, sectioned, and H&E stained. *(A)* Representative lung tissue sections of uninfected lungs; lungs from infected, PC61-treated mice; or lungs from infected isotype-treated mice. *(B and C)* Lung sections were scored for inflammation (B) and proliferation (C). Data are representative of 2 independent experiments that included 4 mice per group. Error bars indicate mean ± SD. Differences between the histology scoring data were determined by the Mann-Whitney U non-parametric test. *(D)* A whole body pleythsmograph was used to measure airway resistance on a daily basis after challenge. The baseline enhanced pause (Penh) is shown as mean ± SD. Data shown are are representative of 2 independent experiments that included 4 mice per group. *(E)* Weight loss was used as a measure of morbidity on a daily basis after challenge. Data show body weight as a percentage of weight at time of infection. Data are

representative of 2 independent experiments and include 4–5 mice per group. *(F through I)* BAL fluid was harvested and analyzed for the pro-inflammatory cytokines IL-6 (F) and IFNγ (G) and chemokines IP10 (H) and MIG (I). For B, C, F, G, H, and I, differences between groups were determined by student t test. For D and E, significance was determined utilizing a two-way ANOVA. Subsequent analysis of individual timepoint significance was determined by Bonferroni post hoc tests; significance (*) indicates $p < 0.05$.

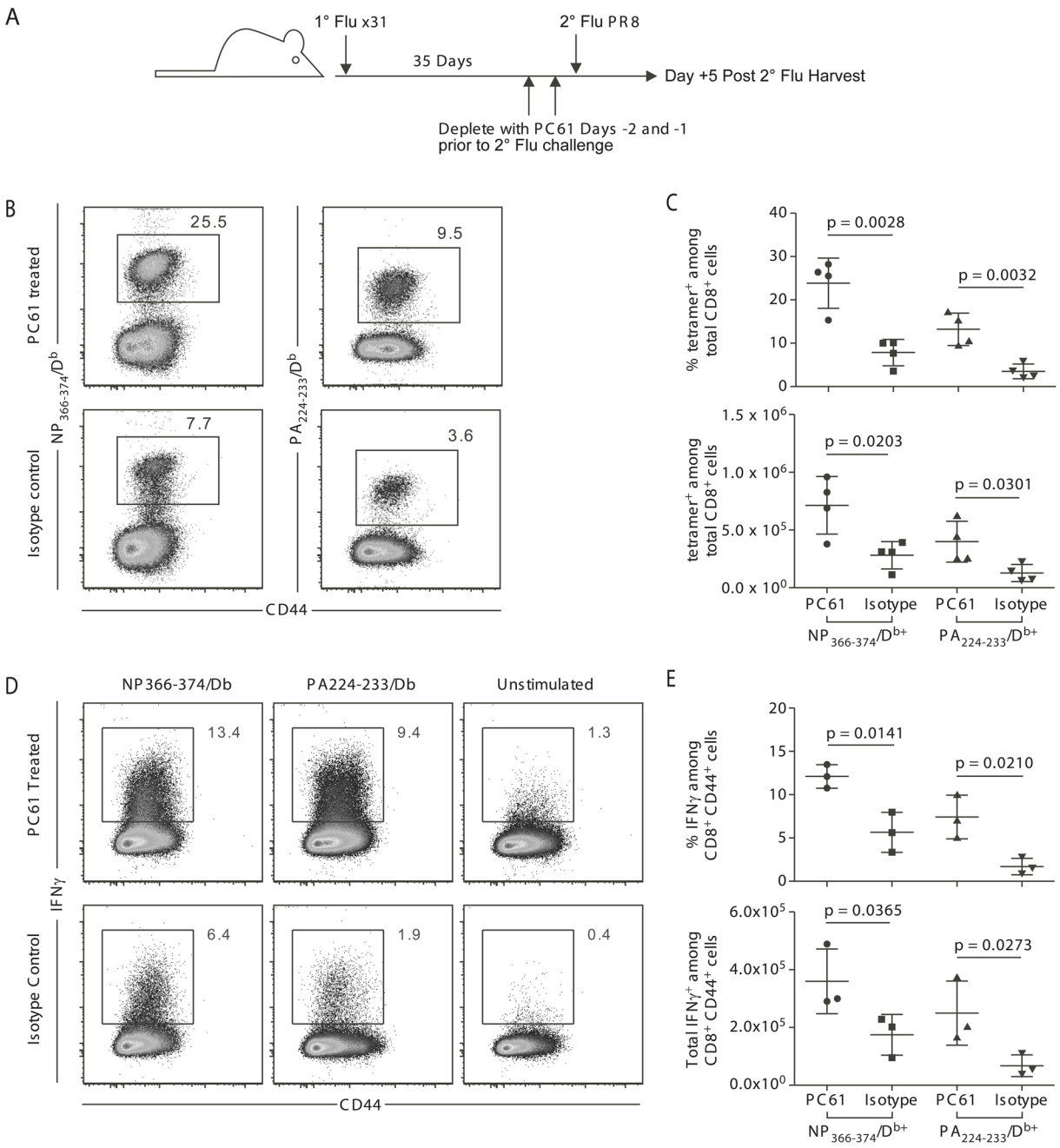

Figure 3. Memory T_{reg} regulate the magnitude of *in vivo* influenza-specific CD8 T cell responses to secondary challenge

C57BL/6 mice were infected with 3000 EID_{50} x31 influenza virus and allowed to rest for 35 days. Mice were treated with PC61 or isotype control, then challenged with 60,000 EID_{50} PR8 influenza virus and sacrificed at day 5 post-infection. *(A)* Schematic of experimental design that outlines infections, antibody treatments, and harvests. *(B and C)* Lymphocytes were isolated from the lungs and stained with influenza NP_{366}/D^b tetramer or PA_{224}/D^b tetramer. (B) Representative staining of influenza-specific CD8 T cell responses in the lung. Plots are gated on $CD8^+$ cells. (C) Percentage of tetramer positive cells among total $CD8^+$ cells in the lung (top panel), and total tetramer positive cells per lung (bottom panel). *(D and*

E) Lymphocytes were isolated from the lungs and analyzed for IFNγ production after peptide stimulation. (D) Representative plots for IFNγ production by $CD8^+$ T cells after stimulation with NP_{366} peptide-pulsed, PA_{224} peptide-pulsed, or unpulsed antigen presenting cells. (E) Percentage of IFNγ positive cells among total $CD8^+$ cells in the lung (top panel). Total IFNγ positive cells per lung (bottom panel). Data points represent individual mice. Lines represent mean. Error bars represent SD. Data are representative of 3 independent experiments. Differences between groups were determined by student t tests.

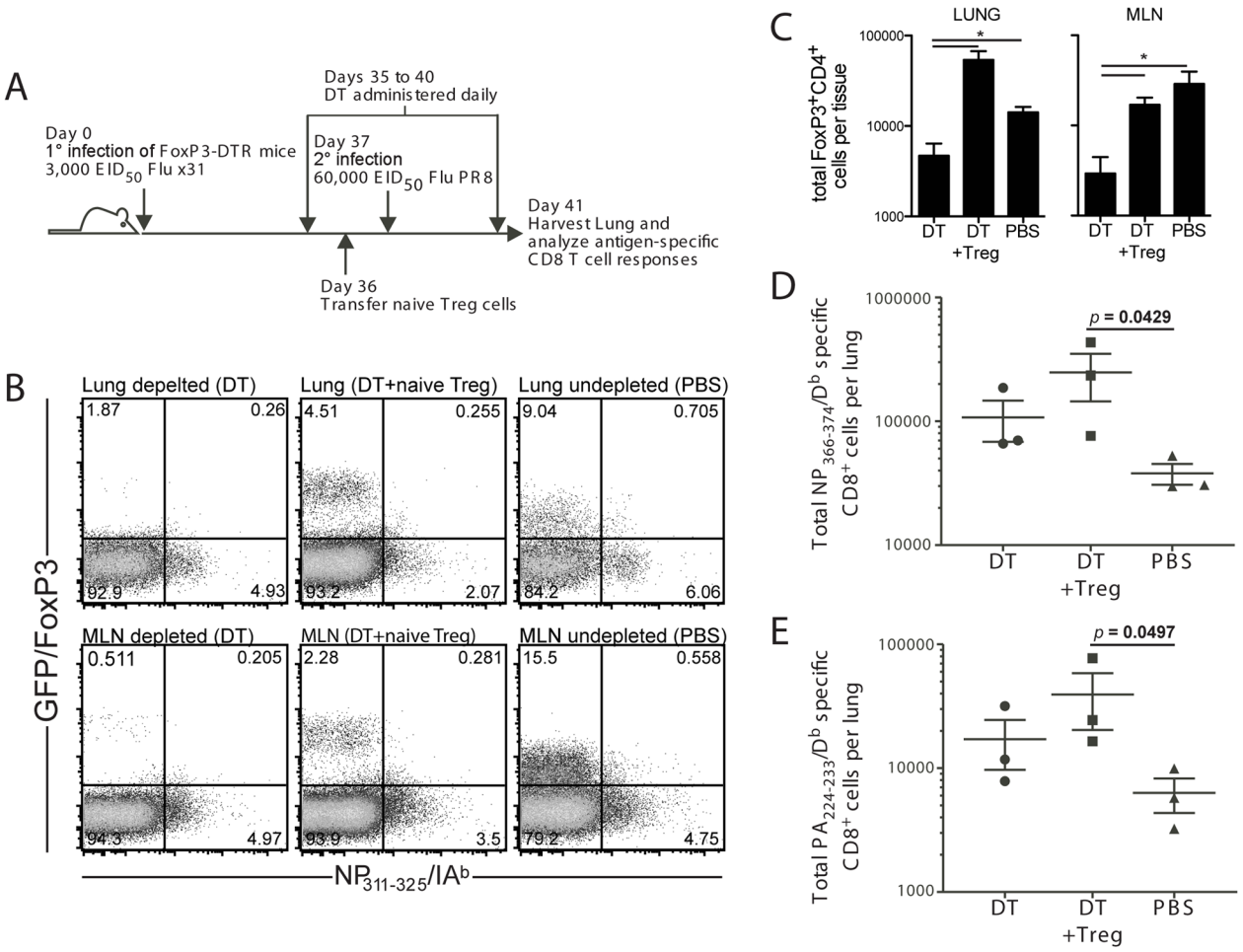

Figure 4. Memory T_{reg} are required to regulate the magnitude of *in vivo* influenza-specific CD8 T cell responses to secondary challenge

FoxP3-DTR mice were infected with 3000 EID_{50} x31 influenza virus and allowed to rest for 35 days. Mice were treated with diphtheria toxin or vehicle, then challenged with 60,000 EID_{50} PR8 influenza virus. In some mice, naïve Treg were adoptively transferred prior to infection. Mice were sacrificed at day 5 post-infection. Lymphocytes were isolated from the lungs and stained with influenza NP_{366}/D^b tetramer or PA_{224}/D^b tetramer. *(A)* Schematic of experimental design that outlines infections, diphtheria toxin treatments, adoptive transfer, and harvest. *(B)* Representative plots from the lung (top row) and dLN (bottom row) gated on total $CD4^+$ cells in tissue harvested from mice treated with diphtheria toxin (DT), treated with diphtheria toxin with a transfer of naïve Treg (DT + Treg), or untreated (PBS). *(C)* Total FoxP3+CD4+ cells per tissue for both the lung (left panel) and the lung-draining lymph node (right panel). *(D)* Total influenza NP_{366}/D^b tetramer positive cells among total $CD8^+$ cells in the lung. *(E)* Total influenza PA_{224}/D^b tetramer positive cells among total $CD8^+$ cells in the lung. Data points in (D) and (E) represent individual mice. Lines represent mean. Error bars represent SD. Data are representative of 2 independent experiments of 3–4 mice per group. Differences between groups were determined by student *t* tests; significance (*) indicates $p < 0.05$.

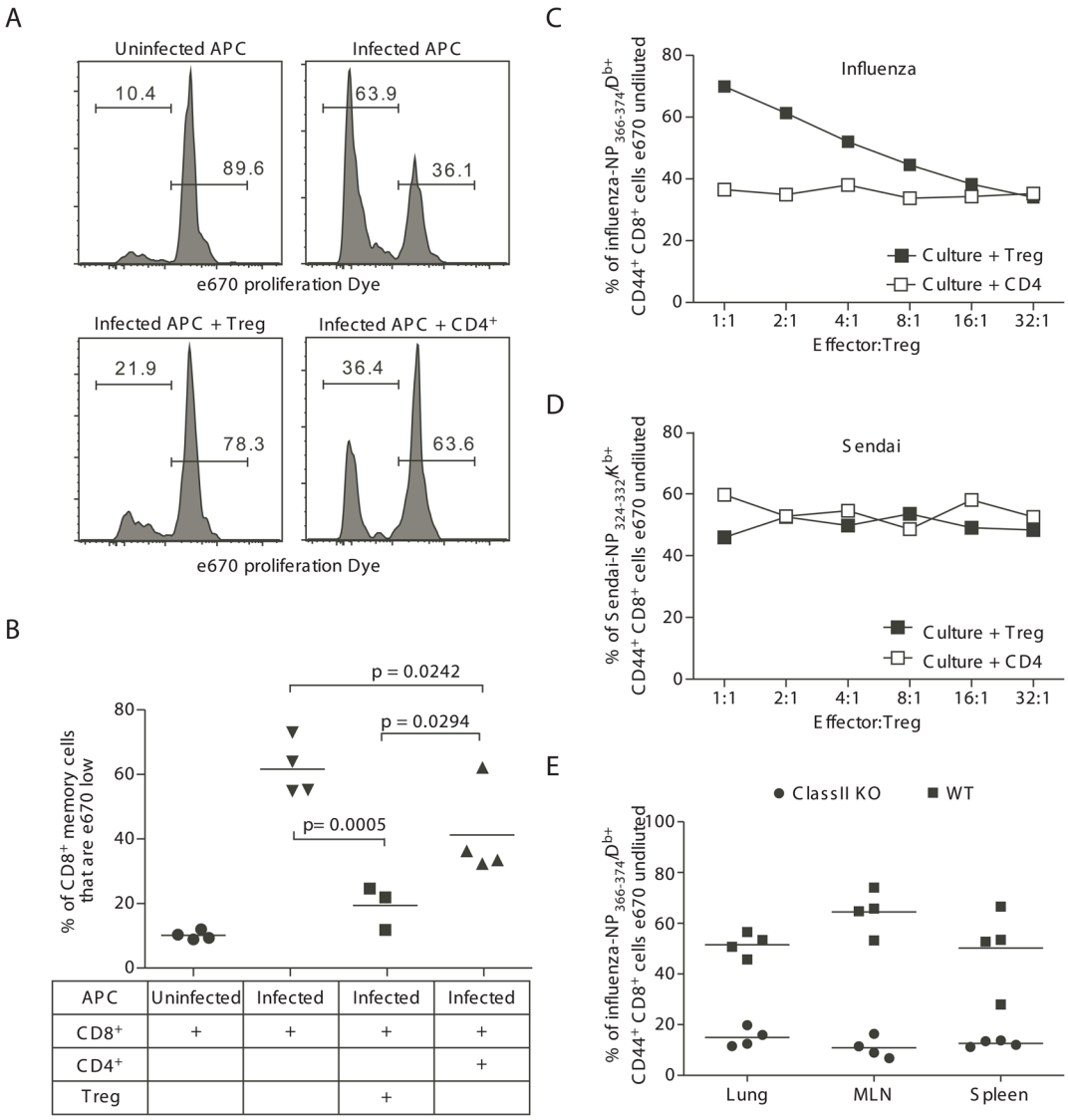

Figure 5. Treg responding to influenza virus challenge inhibit memory T cell proliferation in an antigen-specific fashion

FoxP3-GFP mice were infected with 3000 EID_{50} x31 influenza virus and allowed to rest for 35 days. Mice were then challenged with 60,000 EID_{50} PR8 influenza virus and sacrificed at day 4 post-infection. Lymphocytes were isolated from the lungs, dLN, and spleen, enriched for $CD4^+$ cells, and sorted into GFP^+ (Treg) and GFP^- (CD4 effector) populations and used to inhibit the proliferation of influenza-specific CD8 T cells stimulated with influenza-infected antigen-presenting cells. *(A)* Representative histograms demonstrating the inhibition of CD8 T cell proliferation when Treg are added to wells. Histogram plots are gated on congenic marker$^+$$CD8^+$ cells. *(B)* The frequency of total $CD8^+$ effector cells that had proliferated after co-culture with influenza-infected antigen-presenting cells. Data points represent individual wells; bar represents mean. Data in A and B are representative of 2 independent experiments, in which cells were pooled from 12–15 FoxP3-GFP mice for each experiment. *(C and D)* To assess proliferation of antigen-specific CD8 T cells, influenza-specific Treg were used to suppress proliferation of either influenza-specific CD8 T cells (in C) or Sendai virus-specific CD8 T cells (in D). To identify antigen-specific effector T cells,

cells from proliferation assays were stained with influenza NP_{366}/D^b tetramer (in C) or Sendai $NP_{324}K^b$ tetramer (in D). The frequency of tet^+CD8^+ that had not proliferated is displayed for each ratio of CD8:Treg (■) or CD8:CD4 (□). Data from C and D are concatenated from 4–5 wells for each ratio. Data in C and D are representative of 3 independent experiments, in which cells were pooled from 12–15 FoxP3-GFP mice for each experiment. *(E)* To assess the requirement of MHC Class II for Treg function, influenza-specific Treg from lung, dLN, or spleen were used to suppress proliferation of influenza-specific CD8 T cells in cultures with influenza-infected WT (■) or ClassII knockout (●) antigen-presenting cells. Cells from proliferation assays were stained with influenza NP_{366}/D^b tetramer. The frequency of tet^+CD8^+ that had not proliferated is displayed for each tissue. Data points represent individual wells; bar represents mean. Data in E are representative of 3 independent experiments, in which cells were pooled from 12–15 FoxP3-GFP mice for each experiment.